

A novel Dual Chiral Density Wave in nuclear matter based on a parity doublet structure

Yusuke Takeda,¹ Hiroaki Abuki,² and Masayasu Harada¹

¹*Department of Physics, Nagoya University, Nagoya, 464-8602, Japan*

²*Department of Education, Aichi University of Education, Kariya, 448-8542, Japan*

We study the Dual Chiral Density Wave (DCDW) in nuclear matter using a hadronic model with the parity doublet structure. We first extend the ordinary DCDW ansatz so as to incorporate the effect of an explicit chiral symmetry breaking. Then via numerically evaluating and minimizing the effective potential, we determine the phase structure. We find, in addition to the ordinary DCDW phase where the space average of the chiral condensate vanishes, a new DCDW phase (sDCDW) with a nonvanishing space average depending on the value of the chiral invariant mass parameter.

I. INTRODUCTION

Last few decades, the phase structure of QCD has been one of the main concerns regarding the physics of strong interaction. For the baryon chemical potential lower than the nucleon mass minus binding energy per baryon in nuclei, the phase realized in nature is the QCD vacuum where the chiral symmetry is spontaneously broken. The chiral symmetry breaking is responsible for the mass generation of hadrons as well as the mass splittings of chiral partners.

At sufficiently large chemical potential and/or temperature, the chiral symmetry is expected to restore. An interesting possibility arises when one allows the chiral condensate to vary in space; Nakano and Tatsumi demonstrated in [1] using the NJL model that the symmetry restoration may take place via several steps; going up in density from the vacuum, the system first goes into an intriguing state named as dual chiral density wave (DCDW), that is, a particular type of inhomogeneous chiral phases, making a spiral in the (σ_0, π_0) chiral plane along z direction. Up to present, various inhomogeneous chiral phases are discussed. These includes the real kink crystal (RKC) phase belonging to another class of inhomogeneous phases [2]. In both cases, the chiral symmetry is partially restored in either the momentum space (DCDW) or the real space (RKC). Such inhomogeneous chiral phases may be realized in the neutron stars and may lead to some interesting astrophysical implications [3, 4].

There are number of approaches to chiral inhomogeneous phases. One of the major strategies is to apply the mean-field approximation [5–8] or the Ginzburg-Landau (gradient) expansion [9–11] to the quark-based models such as NJL-type models or quark-meson model [12]. Recently a self-consistent mean-field framework has also been applied [13]. One of the advantages of this kind of approach is that these models are capable of realizing the QCD vacuum properties as well as the color-flavor locked phase of quark matter which is known to be the densest phase of QCD [14]. On the other hand, the main disadvantage is the lack of the ability to reproduce the normal nuclear matter, the QCD phase next to the vacuum phase, followed right after the liquid-gas phase tran-

sition. A quite different approach was taken recently in [15]. Using the parity doublet hadron model tuned to reproduce the bulk properties of normal nuclear matter, the authors have shown that the DCDW phase appears at density several times larger than the normal nuclear density.

In the present paper, we adopt a hadronic model with parity doublet structure (mirror assignment) [16, 17], with vector mesons included in a manner guided by the hidden local symmetry [18, 19]. With the six-point scalar interaction included, the model is known to successfully reproduce bulk properties of normal nuclear matter for a wide range of chiral invariant mass [20]. Our main concerns here are, 1) if the inhomogeneous chiral phase is possible or not within our model, 2) how phase transition points, if any, as a function of μ_B , change with the chiral invariant mass, and 3) what is the effect of current quark mass on the inhomogeneous chiral phase. In particular, the point 3) was missed in [15]. In order to incorporate this in our analyses, we extend the ansatz for the DCDW phase so as to take into account the effect of the explicit symmetry breaking. The extended ansatz smoothly interpolates between the DCDW phase and a nearly symmetry-restored phase. With this setup, we construct the effective potential by diagonalizing the Bogoliubov-de Gennes (BdG) Hamiltonian for nucleons, and determine phases via numerically minimizing the potential. Our main finding is the emergence of another type of DCDW phase which occupies the lower density region according to the value of chiral invariant mass.

The paper is organized as follows. In Sec. II, we describe our model setup and approximation scheme. In Sec. III, we present our numerical results for phases and discuss the phase structure in the plane of μ_B and chiral invariant mass. Sec. IV summarizes the present work.

II. MODEL

In our analysis, we introduce $N^*(1535)$ as the chiral partner to the ordinary nucleon based on the parity doublet structure [16, 17]. For constructing a relativistic mean field model to describe nuclear matter, following Ref. [20], we include ω meson using the hidden local sym-

metry [18, 19] in addition to the scalar and pseudoscalar mesons. The baryon part of the Lagrangian is expressed as [20]

$$\begin{aligned}
\mathcal{L}_N = & \bar{\psi}_{1r} i\gamma^\mu D_\mu \psi_{1r} + \bar{\psi}_{1l} i\gamma^\mu D_\mu \psi_{1l} \\
& + \bar{\psi}_{2r} i\gamma^\mu D_\mu \psi_{2r} + \bar{\psi}_{2l} i\gamma^\mu D_\mu \psi_{2l} \\
& - m_0 [\bar{\psi}_{1l} \psi_{2r} - \bar{\psi}_{1r} \psi_{2l} - \bar{\psi}_{2l} \psi_{1r} + \bar{\psi}_{2r} \psi_{1l}] \\
& - g_1 [\bar{\psi}_{1r} M^\dagger \psi_{1l} + \bar{\psi}_{1l} M \psi_{1r}] \\
& - g_2 [\bar{\psi}_{2r} M \psi_{2l} + \bar{\psi}_{1l} M^\dagger \psi_{2r}] \\
& + a_{\rho NN} [\bar{\psi}_{1l} \gamma^\mu \xi_L^\dagger \hat{\alpha}_{\parallel\mu} \xi_L \psi_{1l} + \bar{\psi}_{1r} \gamma^\mu \xi_R^\dagger \hat{\alpha}_{\parallel\mu} \xi_R \psi_{1r}] \\
& + a_{\rho NN} [\bar{\psi}_{2l} \gamma^\mu \xi_R^\dagger \hat{\alpha}_{\parallel\mu} \xi_R \psi_{2l} + \bar{\psi}_{2r} \gamma^\mu \xi_L^\dagger \hat{\alpha}_{\parallel\mu} \xi_L \psi_{2r}] \\
& + a_{0NN} \text{tr}[\hat{\alpha}_{\parallel\mu}] (\bar{\psi}_{1r} \gamma^\mu \psi_{1r} + \bar{\psi}_{1l} \gamma^\mu \psi_{1l} \\
& + \bar{\psi}_{2r} \gamma^\mu \psi_{2r} + \bar{\psi}_{2l} \gamma^\mu \psi_{2l})
\end{aligned} \tag{1}$$

The part for the scalar and pseudoscalar mesons meson part is given by

$$\begin{aligned}
\mathcal{L}_M = & \frac{1}{4} \text{tr} [\partial_\mu M \partial^\mu M^\dagger] + \frac{1}{4} \bar{\mu}^2 \text{tr} [MM^\dagger] \\
& - \frac{1}{16} \lambda_4 (\text{tr} [MM^\dagger])^2 + \frac{1}{48} \lambda_6 (\text{tr} [MM^\dagger])^3 \\
& + \frac{1}{4} m_\pi^2 f_\pi \text{tr} [M + M^\dagger]
\end{aligned} \tag{2}$$

In this paper, we omit the kinetic and mass terms for vector mesons. Details of the above Lagrangian terms are seen in [20].

In the present analysis, we adopt the following extended DCDW ansatz

$$\langle M \rangle = M(z) \equiv \delta\sigma + \sigma_0 e^{2ifz\tau^3} \tag{3}$$

where $\delta\sigma$, σ_0 and f are parameters with dimension one, and τ^a ($a = 1, 2, 3$) are the Pauli matrices. Space independent part $\delta\sigma$ accommodates the possibility that the space average of DCDW condensate would get nonvanishing shift into σ -direction due to the explicit chiral symmetry breaking. Applying the mean-field approximation, the Lagrangian for nucleon is cast into

$$\begin{aligned}
\mathcal{L}_N = & \bar{\psi}_1 \left[i \not{\partial} - g_1 \left(\delta\sigma + \sigma_0 e^{2ifz\tau^3\gamma_5} \right) + \gamma^0 \mu_B^* \right] \psi_1 \\
& + \bar{\psi}_2 \left[i \not{\partial} - g_2 \left(\delta\sigma + \sigma_0 e^{-2ifz\tau^3\gamma_5} \right) + \gamma^0 \mu_B^* \right] \psi_2 \\
& - m_0 (\bar{\psi}_1 \gamma_5 \psi_2 - \bar{\psi}_2 \gamma_5 \psi_1)
\end{aligned} \tag{4}$$

where μ_B^* is effective chemical potential which include ω contribution as

$$\mu_B^* = \mu_B - g_{\omega NN} \omega_0.$$

The nucleon contribution to the effective potential can be written as

$$\Omega_N = \frac{i}{V_4} \text{Tr} \text{Log}(i\partial_0 - (\mathcal{H}(z) - \mu_B^*)), \tag{5}$$

where V_4 is the space-time volume and $\mathcal{H}(z)$ is the single particle Bogoliubov-de Gennes (BdG) Hamiltonian defined in the space of fermion bispinor $\psi = (\psi_1, \psi_2)$ as

$$\mathcal{H} = \begin{pmatrix} i\gamma^0 \boldsymbol{\gamma} \cdot \nabla + g_1 \gamma^0 M(z) & m_0 \gamma^0 \gamma_5 \\ -m_0 \gamma^0 \gamma_5 & i\gamma^0 \boldsymbol{\gamma} \cdot \nabla + g_2 \gamma^0 M(z)^* \end{pmatrix}$$

This is nothing but the Dirac Hamiltonian in the presence of a periodic potential field $M(z) (= M(z + \frac{\pi}{f}))$. Then the functional trace in Eq. (5) can be evaluated by finding eigenvalues of the operator $\mathcal{H}(z)$ [21]. The eigenvalue has a discrete label as well as continuous three-momentum \mathbf{p} in addition to internal quantum numbers; This is because of the Bloch theorem which states that the eigenfunctions in the presence of a periodic potential are the modified plane wave; the plane wave distorted by periodic functions. To be specific, we decompose the bispinor as

$$\psi(\mathbf{x}) = \sum_{\ell=-\infty}^{\infty} \sum_{\mathbf{p}} \psi_{\mathbf{p},\ell} e^{i(\mathbf{K}_\ell + \mathbf{p}) \cdot \mathbf{x}}$$

where $\mathbf{K}_\ell = (0, 0, 2f\ell)$ is the reciprocal lattice vector. Moving on to the quasimomentum base $\{\psi_{\mathbf{p},\ell}\}$, the BdG Hamiltonian for proton ($I_3 = +1/2$) sector is cast into the following block-diagonalized form:

$$\begin{aligned}
H_{\ell\ell'}(\mathbf{p}) = & \begin{pmatrix} H_{\ell\ell'}^1 & \gamma^0 \gamma_5 m_0 \delta_{\ell\ell'} \\ -\gamma^0 \gamma_5 m_0 \delta_{\ell\ell'} & H_{\ell\ell'}^2 \end{pmatrix} \\
H_{\ell\ell'}^1 = & [(\mathbf{p} + \mathbf{K}_\ell) \cdot \gamma^0 \boldsymbol{\gamma} + g_1 \delta\sigma \gamma^0] \delta_{\ell\ell'} \\
& + g_1 \sigma_0 \gamma^0 [P_r \delta_{\ell\ell'+1} + P_l \delta_{\ell\ell'-1}] \\
H_{\ell\ell'}^2 = & [(\mathbf{p} + \mathbf{K}_\ell) \cdot \gamma^0 \boldsymbol{\gamma} + g_2 \delta\sigma \gamma^0] \delta_{\ell\ell'} \\
& + g_2 \sigma_0 \gamma^0 [P_r \delta_{\ell\ell'-1} + P_l \delta_{\ell\ell'+1}]
\end{aligned}$$

where $P_{r,l}$ is projection operator defined as

$$P_r = \frac{1 + \gamma_5}{2}, \quad P_l = \frac{1 - \gamma_5}{2}.$$

Since the isospin remains a good quantum number, we can simply double the proton contribution in the full effective potential. Then omitting the antiprotons which would not contribute at zero temperature, and diagonalizing $H_{\ell\ell'}(\mathbf{p})$ results in an infinite tower of eigenvalues at each \mathbf{p} , which repeatedly appears for every Brillouin Zone (BZ), $\mathbf{p} \rightarrow \mathbf{p} + \mathbf{K}_\ell$ ($\ell = \dots, -1, 0, 1, \dots$):

$$\sum_{\ell'} H_{\ell\ell'}(\mathbf{p}) \psi_{n,\mathbf{p},\ell'}^{(i)} = E_{n,\mathbf{p}}^{(i)} \psi_{n,\mathbf{p},\ell}^{(i)} \quad (n = 0, 1, \dots, \infty),$$

with $i(=1, 2, 3, 4)$ labeling the internal quantum number (p, p^*) \otimes (\uparrow, \downarrow), where p^* implies the $I_3 = +1/2$ part of $N^*(1535)$. Equation (5) is now evaluated as

$$\Omega_N = \sum_{n=0}^{\infty} \sum_{i=1}^4 \int_{-f}^f \frac{dp_z}{\pi} \int \frac{d\mathbf{p}_\perp}{(2\pi)^2} (E_{n,\mathbf{p}}^{(i)} - \mu_B^*) \theta(\mu_B^* - E_{n,\mathbf{p}}^{(i)}) \tag{6}$$

with $\mathbf{p}_\perp = (p_x, p_y, 0)$. The following meson contributions add up to the full expression of the thermodynamic potential.

$$\begin{aligned}\Omega_M = & -\frac{1}{2}m_\omega^2\omega_0^2 - \frac{1}{2}\bar{\mu}^2(\delta\sigma^2 + \sigma_0^2) + 2\sigma_0^2f^2 \\ & + \frac{1}{4}\lambda_4[(\delta\sigma^2 + \sigma_0^2)^2 + 2\delta\sigma^2\sigma_0^2] \\ & - \frac{1}{6}\lambda_6[(\delta\sigma^2 + \sigma_0^2)^3 + 6(\delta\sigma^2 + \sigma_0^2)\delta\sigma^2\sigma_0^2] \\ & - m_\pi^2f_\pi\delta\sigma.\end{aligned}\quad (7)$$

The feedback from an explicit chiral symmetry breaking is taken care by the last term.

Assuming for a while the existence of normal nuclear matter within the model, model parameters except for chiral invariant mass for nucleon are determined by the pion decay constant $\sigma_0 = f_\pi = 92.2$ MeV in vacuum, baryon and meson masses shown in Table I and normal nuclear property shown in Table II. In homogeneous phase the baryon mass is calculated as

$$m_\pm = \frac{1}{2} \left[\sqrt{(g_1 + g_2)^2 \sigma_0^2 + 4m_0^2} \mp (g_1 - g_2) \sigma_0 \right]. \quad (8)$$

The determined parameters are summarized in Table III. However, we will show later that the normal nuclear matter exists only as a metastable state as another type of DCDW phase dominates over it once chiral invariant mass becomes smaller than some critical value, $m_0 \lesssim 800$ MeV.

TABLE I. Values of baryon and meson mass in unit of MeV

m_+	m_-	m_π	m_ω
939	1535	140	783

TABLE II. Physical inputs in normal nuclear density

Saturation density	ρ_0	0.16 [fm ⁻³]
Binding energy	$\frac{E}{A} - 939$	-16 [MeV]
Incompressibility	K	240 [MeV]

TABLE III. Determined parameters for given chiral invariant mass

m_0	500	600	700	800	900
g_1	9.03	8.49	7.82	7.00	5.97
g_2	15.5	15.0	14.3	13.5	12.4
$g_{\omega NN}$	11.3	9.13	7.30	5.66	3.52
$\bar{\mu}$ [MeV]	441	437	406	320	114
λ_4	42.2	40.6	35.7	23.2	4.47
$\lambda_6 \cdot f_\pi^2$	17.0	15.8	14.0	8.94	0.644

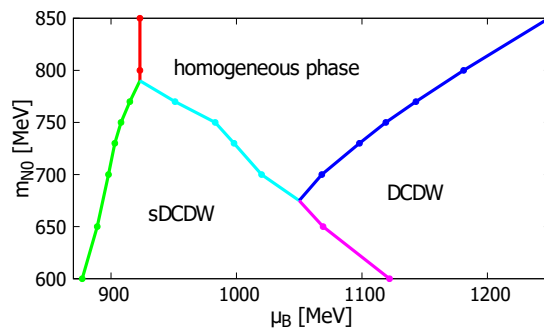


FIG. 1. Phase structure in $\mu_B - m_0$ plane.

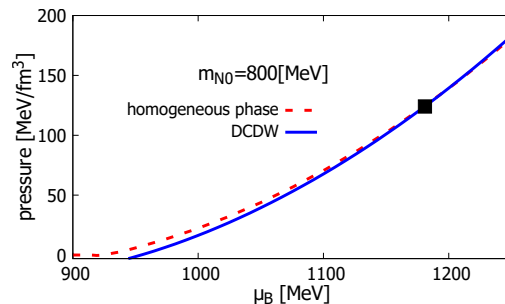


FIG. 2. Relation between chemical potential and pressure for $m_0 = 800$ MeV. The blue solid curve and red dashed curve show DCDW phase and homogeneous phase, respectively. The point of phase transition from the homogeneous phase to the DCDW phase is expressed by black square.

III. PHASE STRUCTURE

The phase diagram can be obtained by numerically solving the stationary conditions of thermodynamic potential for f , $\delta\sigma$, σ_0 and ω_0 .

In Figure 1, we show the phase structure in $\mu_B - m_0$ plane. We find that there exist two kinds of DCDW phase: the ordinary DCDW phase indicated as “DCDW” and a new DCDW phase as “sDCDW”.

In the following, we discuss the phases and the associated phase transitions in detail for two typical cases (a) $m_0 = 800$ MeV, and (b) $m_0 = 700$ MeV.

a. $m_0 = 800$ MeV. Figure 2 shows the pressure for the homogeneous ($f = 0$, a dashed curve) and DCDW states ($f \neq 0$, a solid curve) as a function of μ_B in this case. These two states consist only two stationary solutions for $\delta\Omega = 0$ for a given value of μ_B . The DCDW state found here corresponds to the ordinary DCDW state in nuclear matter [15], but here the chiral condensate $M(z)$ has a finite offset $\delta\sigma$ due to an explicit symmetry breaking. The ordinary DCDW state takes over the homogeneous nuclear matter at $\mu_B \sim 1200$ MeV denoted in the figure by square.

In what follows, for the comparison with the ordinary

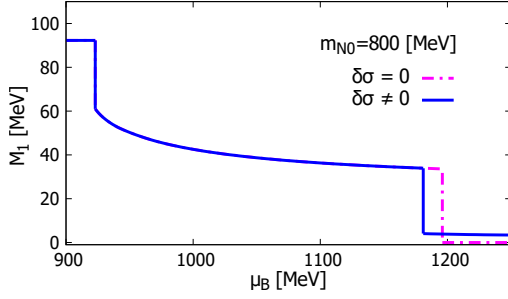


FIG. 3. Relation between chemical potential and M_1 for $m_0 = 800$ MeV. The blue solid curve and magenta dot-dashed curve show the configuration of the extended ansatz with $\delta\sigma \neq 0$ and the ordinary ansatz with $\delta\sigma = 0$, respectively.

ansatz, we define the thermodynamic potential with the condition $\delta\sigma = 0$ is forced by

$$\Omega_0 = \Omega|_{\delta\sigma=0}.$$

Figure 3 shows one of order parameter M_1 defined by

$$M_1 \equiv \frac{1}{2V} \int_{-\infty}^{\infty} d^3x \text{tr} [\langle M \rangle] = \begin{cases} \delta\sigma + \sigma_0 & (f = 0) \\ \delta\sigma & (f \neq 0) \end{cases} \quad (9)$$

This quantity may be regarded roughly as a guide for the strength of chiral symmetry breaking. We see that solid curve in the region of the DCDW phase is nonvanishing, indicating that the effect of explicit symmetry breaking is properly taken into account in our extended ansatz.

Depicted in Figure 4 is the wave number f as a function of μ_B . The quantity provides a guide for a translational symmetry breaking. We note that, even though the effect of $\delta\sigma$ gives a minor effect on the magnitude of f , it brings about a sizable shift of the critical chemical potential, making the onset point several tens of MeV earlier than the case of ordinary ansatz. Figure 5 shows the baryon density in the unit of normal nuclear density as a function of μ_B . We read the DCDW onset density as $\rho_B^c \sim 4.7\rho_0$. This value is larger than the one in Ref. [15]. We would like to stress that the stable DCDW phase, on the other hand, appears already at $\rho_B \sim 4.8\rho_0$, while the stable phase appears at $\rho_B \sim 10.4\rho_0$ in Ref. [15]. This means that the magnitude of density jump from the uniform state to the DCDW phase is smaller and therefore the strength of the first order phase transition is weaker in our case. We think that one of the reasons is that the chiral invariant mass is independent of μ_B , while it depends in the model used in Ref. [15].

b. $m_0 = 700$ MeV. Next, we show the μ_B dependence of the pressure for $m_0 = 700$ MeV in Fig. 6. We first notice that in this case the normal nuclear matter exists only as a metastable state. This is due to the

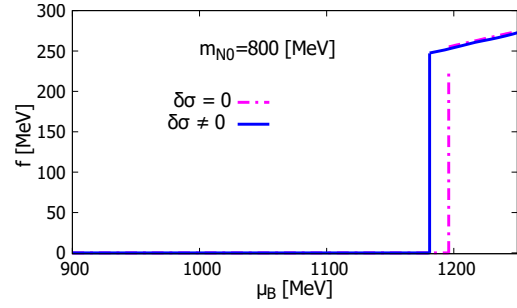


FIG. 4. Relation between chemical potential and f for $m_0 = 800$ MeV. The blue solid curve and magenta dot-dashed curve show the configuration of the extended ansatz with $\delta\sigma \neq 0$ and the ordinary ansatz with $\delta\sigma = 0$, respectively.

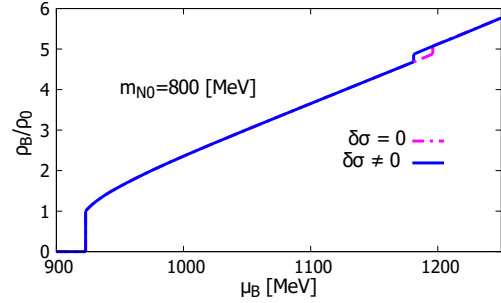


FIG. 5. Relation between chemical potential and f for $m_0 = 800$ MeV. The blue solid curve and magenta dot-dashed curve show the configuration of the extended ansatz with $\delta\sigma \neq 0$ and the ordinary ansatz with $\delta\sigma = 0$, respectively.

emergence and the stabilization of a new DCDW state: in addition to the ordinary DCDW phase, we find another solution with $f \neq 0$ which is shown by dotted curve in Fig. 6. To distinguish two solutions with $f \neq 0$, we call this phase the shifted DCDW (sDCDW) phase for a reason described shortly. We plot the μ_B dependence of M_1 defined in Eq. (9) in Fig. 7, and that of f in the DCDW phase in Fig. 8.

From the former, we see that, going up in density, the chiral symmetry restores via several steps. From the latter, we clearly see that there are two regions of DCDW phase: the sDCDW state with $f \sim 50-100$ MeV for $900 \lesssim \mu_B \lesssim 1020$ MeV, and the ordinary DCDW state with $f \gtrsim 220$ MeV for $\mu_B \gtrsim 1070$ MeV. Figure 7 shows that the value of M_1 for $\mu_B \gtrsim 1070$ MeV is less than 10 MeV which is close to the one in the DCDW phase shown in Fig. 3, and so is the value of f ($f \gtrsim 220$ MeV). In fact, this phase is smoothly connected to the ordinary DCDW phase realized for $m_0 = 800$ MeV as is seen from the phase diagram Fig. 1. On the other hand, Fig. 8 shows that the value of f ($f \sim 50-100$ MeV) in the sDCDW phase is less than half of the value in the ordinary DCDW phase shown in Fig. 4. Furthermore,

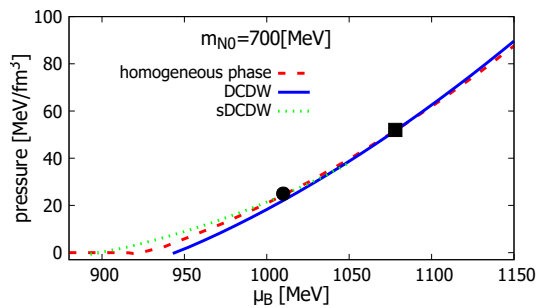


FIG. 6. Relation between chemical potential and pressure for $m_0 = 700$ MeV. The blue solid curve and red dashed curve show the DCDW phase and the homogeneous phase, respectively. The green dotted curve shows the sDCDW which is another solution with $f \neq 0$. The point of phase transition from the homogeneous phase to DCDW phase is expressed by black square, while that from the sDCDW phase to the homogeneous phase is indicated by black circle.

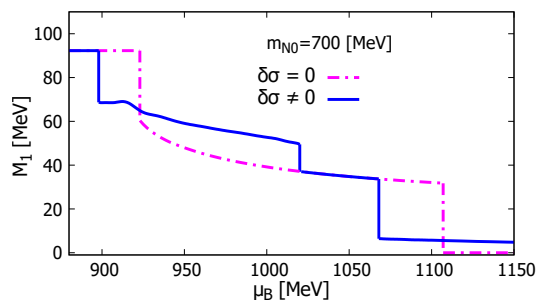


FIG. 7. Relation between chemical potential and M_1 for $m_0 = 700$ MeV. The blue solid curve and magenta dot-dashed curve show the configuration of the extended ansatz with $\delta\sigma \neq 0$ and the ordinary ansatz with $\delta\sigma = 0$, respectively.

Figure 7 shows that the value of M_1 for $900 \lesssim \mu_B \lesssim 1020$ MeV is $M_1 \sim 50\text{--}70$ MeV which is much larger than 10 MeV in the ordinary DCDW phase shown in Fig. 7. Since $M_1 = \delta\sigma$ in the DCDW phase, the large difference of M_1 is caused by the difference of the values of $\delta\sigma$: $\delta\sigma \lesssim 10$ MeV in the ordinary DCDW phase realized for $\mu_B \gtrsim 1070$ MeV, while $\delta\sigma \sim 50$ MeV for $900 \lesssim \mu_B \lesssim 1020$ MeV. This implies that the center of the chiral spiral in the (σ, π^0) chiral plane, which is near origin in the ordinary DCDW phase, is shifted to the σ direction. That is why we called the phase realized for $900 \lesssim \mu_B \lesssim 1020$ MeV the shifted-DCDW (sDCDW) phase. We would like to stress that, on the contrary to the ordinary DCDW phase, the solution of stationary condition for $\delta\sigma$ do not become zero even if it is in chiral limit.

The relation between chemical potential and baryon number density is shown in Fig 9. From the figure, we see that the QCD phase next to the vacuum is the sDCDW phase for $m_0 = 700$ MeV.

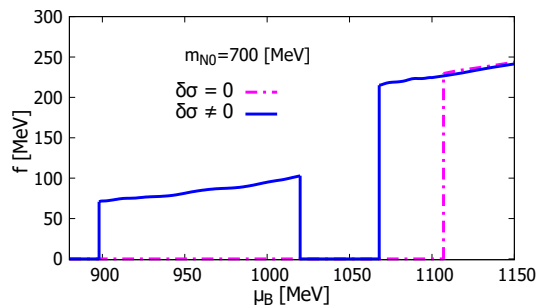


FIG. 8. Relation between chemical potential and wavenumber f for $m_0 = 700$ MeV. The blue solid curve shows the solution under the extended ansatz with $\delta\sigma \neq 0$, while the magenta dot-dashed curve corresponds to the solution with the ordinary ansatz, $\delta\sigma = 0$.

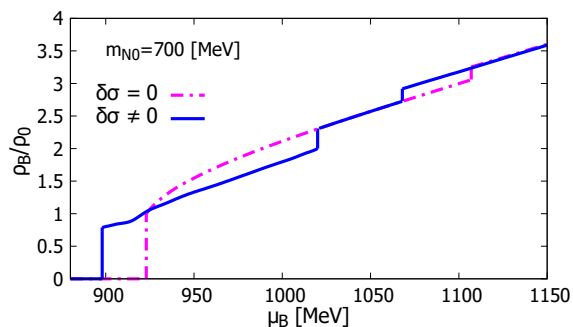


FIG. 9. Relation between chemical potential and baryon number density for $m_0 = 700$ MeV. The blue solid curve and magenta dot-dashed curve show the configuration of the extended ansatz with $\delta\sigma \neq 0$ and the ordinary ansatz with $\delta\sigma = 0$, respectively.

IV. A SUMMARY AND DISCUSSIONS

We studied the inhomogeneous phase structure in nuclear matter using a nucleon-based model with parity doublet structure where $N^*(1535)$ is introduced as the chiral partner of $N(939)$. Adopting the extended ansatz, Eq. (3), we studied the effect of $\delta\sigma$ and found that, depending on the value of the chiral invariant mass m_0 , the sDCDW phase exists in addition to the ordinary DCDW phase.

In the ordinary DCDW phase for large m_0 , the space average of chiral condensate M_1 , Eq. (9), becomes less than 10 MeV, implying that this phase is smoothly connected to the DCDW phase obtained with the familiar ansatz $\delta\sigma = 0$. For $m_0 = 800$ MeV, the critical density from the homogeneous phase to DCDW phase is $4.7\rho_0$. The wave number f has value of $200 \sim 300$ MeV which is in fair agreement with the result obtained in Ref.[15].

On the other hand, when chiral invariant mass $m_0 \lesssim 780$ MeV the sDCDW phase appears at low density. This phase is characterized by a smaller wave number f and a

large shift of chiral condensate, $\delta\sigma$. It is noteworthy that it is not the effect of explicit chiral symmetry breaking but the dynamical symmetry breaking that produces this large shift of chiral condensate. So we expect that this sDCDW phase survives in the chiral limit.

The parameter range of chiral invariant mass where the sDCDW is stabilized, fails to realize nuclear matter as the pressure of sDCDW is so strong that it diminishes the liquid-gas phase transition structure. Then, one might think that the present model for m_0 less than 780 MeV is ruled out. However, the chiral invariant mass m_0 can have density dependence as in Ref. [15] which shows that m_0 decreases against increasing density. In such a case, the sDCDW phase may be realized in high density nuclear matter in the real world.

Exploring the elementary excitations in the sDCDW phase deserves further investigations in future. In the ordinary DCDW phase, apparently both the chiral symmetry and the translational invariance along z -direction are spontaneously broken, but a particular combination of them is left invariant [22, 23]. As a result, the num-

ber of spontaneously broken generator is three which implies that no extra Nambu-Goldstone boson appears other than three pions. In contrast, the combination is also spontaneously broken in the sDCDW phase. Then, we expect that a phonon mode appears in the sDCDW phase which may signal the phase. On the other hand, heavy hadrons may also serve as some interesting hard probes in the sDCDW background [24].

Another interesting extension of current work is to include an external magnetic field. For quark matter, several studies were already devoted to the topic of inhomogeneous phases under the magnetic field [25–30]. In [26], a new DCDW phase was found to occupy the low density region in an arbitrary small magnetic background. They called the phase “weak” DCDW since it has a smaller value of f . Since they did not consider the possible shift of chiral condensate, $\delta\sigma$, the analysis within the nucleon-based model with including both $\delta\sigma$ and magnetic field would be an interesting subject worth exploring.

Acknowledgement. This work was partially supported by JPSP KAKENHI Grant Number JP16K05346 (H.A.) and 16K05345 (M.H.).

-
- [1] E. Nakano and T. Tatsumi, Phys. Rev. D **71**, 114006 (2005).
 - [2] D. Nickel, Phys. Rev. Lett. **103**, 072301 (2009).
 - [3] T. Tatsumi and T. Muto, Phys. Rev. D **89**, no. 10, 103005 (2014) doi:10.1103/PhysRevD.89.103005.
 - [4] M. Buballa and S. Carignano, Eur. Phys. J. A **52**, no. 3, 57 (2016).
 - [5] D. Nickel, Phys. Rev. D **80**, 074025 (2009).
 - [6] S. Carignano, D. Nickel and M. Buballa, Phys. Rev. D **82**, 054009 (2010).
 - [7] P. Adhikari, J. O. Andersen and P. Kneschke, Phys. Rev. D **96**, no. 1, 016013 (2017).
 - [8] S. Karasawa and T. Tatsumi, Phys. Rev. D **92**, no. 11, 116004 (2015).
 - [9] H. Abuki, D. Ishibashi and K. Suzuki, Phys. Rev. D **85**, 074002 (2012).
 - [10] H. Abuki, Phys. Lett. B **728**, 427 (2014).
 - [11] S. Carignano, M. Mannarelli, F. Anzuini and O. Benhar, Phys. Rev. D **97**, no. 3, 036009 (2018).
 - [12] See for a review, M. Buballa and S. Carignano, Prog. Part. Nucl. Phys. **81**, 39 (2015).
 - [13] T. G. Lee, K. Nishiyama, N. Yasutake, T. Maruyama and T. Tatsumi, JPS Conf. Proc. **14**, 020808 (2017).
 - [14] See for example, M. G. Alford, A. Schmitt, K. Rajagopal and T. Schäfer, Rev. Mod. Phys. **80**, 1455 (2008); D. H. Rischke, Prog. Part. Nucl. Phys. **52**, 197 (2004).
 - [15] A. Heinz, F. Giacosa and D. H. Rischke, Nucl. Phys. A **933**, 34 (2015).
 - [16] C. E. Detar and T. Kunihiro, Phys. Rev. D **39**, 2805 (1989).
 - [17] D. Jido, M. Oka and A. Hosaka, Prog. Theor. Phys. **106**, 873 (2001).
 - [18] M. Bando, T. Kugo and K. Yamawaki, Phys. Rept. **164**, 217 (1988).
 - [19] M. Harada and K. Yamawaki, Phys. Rept. **381**, 1 (2003).
 - [20] Y. Motohiro, Y. Kim and M. Harada, Phys. Rev. C **92**, no. 2, 025201 (2015).
 - [21] See for example, D. Nickel and M. Buballa, Phys. Rev. D **79**, 054009 (2009).
 - [22] T. G. Lee, E. Nakano, Y. Tsue, T. Tatsumi and B. Friman, Phys. Rev. D **92**, no. 3, 034024 (2015).
 - [23] Y. Hidaka, K. Kamikado, T. Kanazawa and T. Noumi, Phys. Rev. D **92**, no. 3, 034003 (2015).
 - [24] D. Suenaga and M. Harada, Phys. Rev. D **93**, no. 7, 076005 (2016).
 - [25] I. E. Frolov, V. C. Zhukovsky and K. G. Klimenko, Phys. Rev. D **82**, 076002 (2010).
 - [26] K. Nishiyama, S. Karasawa and T. Tatsumi, Phys. Rev. D **92**, 036008 (2015).
 - [27] R. Yoshiike, K. Nishiyama and T. Tatsumi, Phys. Lett. B **751**, 123 (2015).
 - [28] R. Yoshiike and T. Tatsumi, Phys. Rev. D **92**, no. 11, 116009 (2015).
 - [29] G. Cao and A. Huang, Phys. Rev. D **93**, no. 7, 076007 (2016).
 - [30] H. Abuki, EPJ Web Conf. **129**, 00036 (2016).